

# On-Line Monitoring of Human Prostate Cancer Cells in a Perfusion Rotating Wall Vessel by Near-Infrared Spectroscopy

Martin H. Rhiel,<sup>1</sup> Michael B. Cohen,<sup>2</sup> Mark A. Arnold,<sup>3</sup> David W. Murhammer<sup>1\*</sup>

<sup>1</sup>Department of Chemical and Biochemical Engineering, 4133 Seamens Center, University of Iowa, Iowa City, Iowa 52242; telephone: 319-335-1228; fax: 319-353-1415; e-mail: murham@engineering.uiowa.edu

<sup>2</sup>Department of Pathology, 4133 Seamens Center, University of Iowa, Iowa City, Iowa 52242

<sup>3</sup>Department of Chemistry, 4133 Seamens Center, University of Iowa, Iowa City, Iowa 52242

Received 7 July 2003; accepted 29 September 2003

Published online 11 May 2004 in Wiley InterScience (www.interscience.wiley.com). DOI: 10.1002/bit.10834

**Abstract:** PC-3 human prostate cancer cells have been cultivated in a rotating wall vessel in which glucose, lactate, and glutamine profiles were monitored noninvasively and in real time by near-infrared (NIR) spectroscopy. The calibration models were based on off-line spectra from tissue culture experiments described previously (Rhiel et al., *Biotechnol Bioeng* 77:73–82). Monitoring performance was improved by Fourier filtering of the spectra and initial off-set adjustment. The resulting standard errors of predictions were 0.95, 0.74, and 0.39 mM for glucose, lactate, and glutamine, respectively. The concentration of ammonia could not be accurately measured from the same spectra. In addition, metabolite uptake and production rates were determined for PC-3 prostate cancer cells during exponential growth in batch-mode cultivation. Cells grew with a doubling time of 21 h and consumed glucose and glutamine at rates of 6.8 and  $1.8 \times 10^{-17}$  mol/cell·s, respectively. This resulted in lactate and ammonia production rates of 11.9 and  $1.3 \times 10^{-17}$  mol/cell·s, respectively. Compared with other monitoring technologies, this technology has many advantages for spaceflights and stand-alone units; for instance, calibration can be performed at one time and then applied in a reagentless, low-maintenance way at a later time. The resulting concentration information can be incorporated into closed-loop control schemes, thereby leading to better in vitro models of in vivo behavior. © 2004 Wiley Periodicals, Inc.

**Keywords:** rotating wall vessel; on-line monitoring; near-infrared spectroscopy; PC-3 human prostate cancer cells

## INTRODUCTION

Advancement of cell cultures for in vitro modeling of in vivo conditions requires close simulation of in vivo conditions.

Correspondence to: D. W. Murhammer

\*Current address: Process Development, Cytos Biotechnology AG, Zürich-Schlieren, Switzerland

Contract grant sponsor: Microgravity Science and Applications Division of the National Aeronautics and Space Administration

Contract grant number: NAG8-1592

Often, key features of in vivo conditions are three-dimensional (3D) growth and tight metabolic control. Designing bioreactor systems that address these features is a challenge.

Recently, rotating wall vessels (RWVs) developed at the National Aeronautics and Space Administration/Johnson Space Center (NASA/JSC) (Wolf and Schwarz, 1991,1992) have been used to culture various cell types, including *Escherichia coli* (Fang et al., 1997a, 2000), *Streptomyces clavuligerus* (Fang et al., 1997b), insect cells (Francis et al., 1997; Saarinen and Murhammer, 2000), baby hamster kidney cells (Schwarz et al., 1992), neuron-like cells (Lelkes et al., 1998; Wang and Good, 2001), epithelial cells (Chopra et al., 1997; Jessup et al., 1994), erythroid cells (Sytkowski and Davis, 2001), colon carcinoma (Goodwin et al., 1992), mixed müllerian tumor of the ovary (Goodwin et al., 1997), prostate cancer cells (Ingram et al., 1997; Winkenwerder et al., 2003), HeLa cells (Long et al., 1998), skeletal muscle satellite cells (Molnar et al., 1997), skeletal and cardiovascular tissues (Bursac et al., 1999; Sutherland et al., 2002), lymphoid tissue (Margolis et al., 1997), and stem cells (Colvin et al., 2002). The observed advantages are mainly the formation of 3D aggregates and differentiation into tissue-like structures that mimic in vivo characteristics (Bursac et al., 1999; Goodwin et al., 1997; Ingram et al., 1997; Klement and Spooner, 1993; Schwarz et al., 1992). This approach has been exploited extensively for bone tissue engineering (Baker and Goodwin, 1997; Duke et al., 1993, 1996; Granet et al., 1998; Ontiveros and McCabe, 2003; Qiu et al., 1999, 2001; Radin et al., 2001; Rucci et al., 2002), lymphoid tissue (Cooper and Pellis, 1998; Cooper et al., 2001; Licato and Grimm, 1999; Long and Hughes, 2001; Margolis et al., 1997; Sastry et al., 2001), and prostate cancer cell modeling (Clejan et al., 1996, 2001; Ingram et al., 1997; Margolis et al., 1999; O'Connor et al., 1997; Zhau et al., 1997).

Although the RWV provides an excellent system for growing 3D aggregates, it should be emphasized that on-line

monitoring and control systems for this type of bioreactor are uncommon. In addition, utilization of RWVs during spaceflight missions necessitates long-term stable sensor systems with minimal maintenance requirements. Previously described on-line monitoring systems for RWVs include pH monitoring (Jeevarajan et al., 2002) and glucose monitoring (Xu et al., 2002). Using the amperometric glucose sensor described by Xu et al. (2002), it was possible to monitor glucose continuously for 16 days while using a single calibration and for 30 days using two sets of calibrations. Their reported standard error of prediction (SEP) was 0.5 mM (Xu et al., 2002).

Glucose is a necessary nutrient for cell cultures, but it is not the only nutrient contained in the cell culture medium. Glutamine, for example, is also necessary and thus it too is important (Zielke et al., 1978). In addition, the waste products of the cellular metabolism are also important as they may accumulate to toxic levels when the nutrient concentration is not controlled (Glacken et al., 1986). For this reason, Rhiel et al. (2002a) investigated whether four key metabolites (glucose, lactate, glutamine, and ammonia) could be monitored with near-infrared (NIR) spectroscopy. The advantage of spectroscopic sensors is that multiple components can be measured simultaneously and non-invasively (Rhiel et al., 2002a). Simultaneous measurement eliminates the need for multiple sensors, and noninvasive measurement avoids the need for elaborate sterilizations, such as, for example, with the amperometric sensor described by Xu et al. (2002). Rhiel et al. (2002a) generated calibration models able to monitor glucose, lactate, glutamine, and ammonia with SEPs of 0.82, 0.94, 0.55, and 0.76 mM, respectively (Rhiel et al., 2002a). Similar results were obtained by Zhou et al. (1995), Chung et al. (1996), Riley et al. (1997, 1998a, 1998b), McShane and Coté (1998), and Lewis et al. (2000) for cell cultures, and Cavinato et al. (1990), Ge et al. (1994), Hall et al. (1996), and Yano et al. (1998) for fermentations. Thus, a sensor system based on NIR spectroscopy seems to be suitable for RWV monitoring.

The goal of the present work was to investigate the on-line monitoring of RWVs using NIR spectroscopy, specifically the on-line monitoring of cultivations of PC-3 human prostate cancer cells from established calibration models. A priori establishment of calibration models is particularly desired for spaceflight missions as the system could be calibrated on earth and operated with minimal input during the subsequent flight. In general, a priori-established calibration models are useful for frequent subsequent cultivations when operator time and costs are to be minimized. For example, Rhiel et al. (2002b) described the establishment of one-time calibration models, which were still valid after 2 to 3 years. The calibration models were established using randomly spiked off-line tissue culture samples. This adaptive calibration approach yields more robust calibration models (Rhiel et al., 2002c) and was used as a basis in this work. In fact, basic calibration model development has been described previously (Rhiel et al., 2002a).

## MATERIALS AND METHODS

### Cell Line, Medium, and Microcarriers

PC-3 human prostate cancer cells (ATCC CRL 1435) were grown in RPMI-1640 medium (Gibco, Grand Island, NY) supplemented with 10% fetal bovine serum (FBS; Gibco), 2 mM glutamine, 0.1 mM 2-mercaptoethanol, 100 mg/mL streptomycin, and 100 U/mL penicillin (Rokhlin and Cohen, 1995). In general, cells were maintained in T-75 tissue culture flasks (Corning, Inc., Corning, NY) containing 10 mL medium and expanded to inoculate T-150 tissue culture flasks (Corning) containing 15 mL of medium (Rhiel et al., 2002a). Each perfusion RWV experiment was inoculated at a viable density of  $2 \times 10^5$  cells/mL. In addition, Cytodex 3 microcarriers (Sigma Chemical Co., St. Louis, MO) were added at a concentration of 5 mg/mL to provide an attachment surface.

### Bioreactor

A perfusion RWV (pRWV) with a 125-mL vessel volume, equipped with a silicone membrane oxygenator, peristaltic pump, and liquid handling manifold, was purchased from Synthecon, Inc. (Houston, TX). Schematics of the experimental set-ups are shown in Figure 1 for batch (fed-)batch and continuous perfusion operation. The spent medium outlet at the inner cylinder of the pRWV was covered with a 100- $\mu$ m mesh size polypropylene filter to retain cells attached to microcarriers. Unless otherwise noted, the

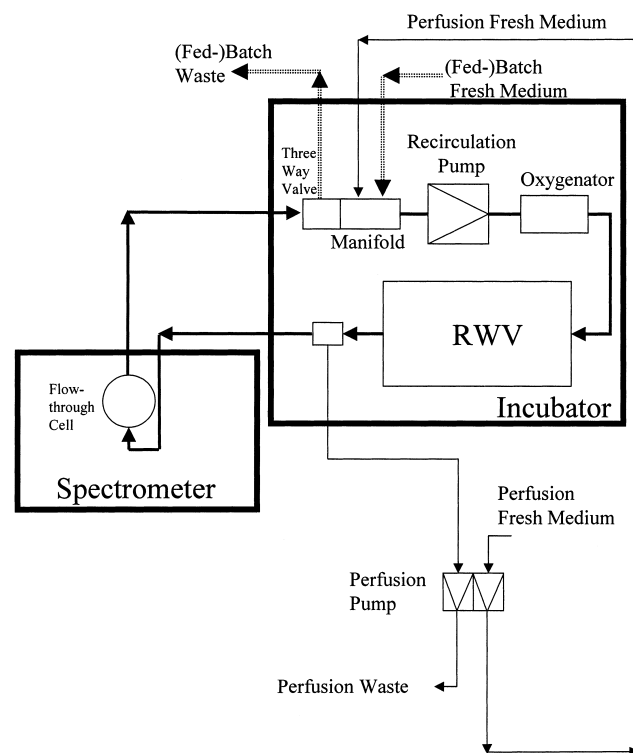


Figure 1. Perfusion RWV setup.

culture medium in the pRWV was recirculated through the oxygenator at a constant flowrate of 16 mL/min. The pRWV was operated inside a humidified 37°C incubator with a 5% CO<sub>2</sub> atmosphere utilizing methods adapted from Schwarz et al. (1992). Unless noted otherwise, both the inner and outer cylinder of the pRWV were rotated at the same speed of 25 rpm. The set-up of the pRWV provided by the manufacturer allowed only manual "infusion" of fresh medium intended for a limited amount of time using a syringe attached to the manifold (Fig. 1). For continuous perfusion experiments the system was modified by connecting a low-flowrate multistaltic pump (LabConco, Kansas City, MO) to supply fresh medium and withdraw spent medium continuously (Fig. 1). The spent medium line leaving the system was connected to the head of the LabConco pump to the outward direction with the same size tubing as the fresh medium line. Thus, equal volumes could enter and leave the system. To account for potential differences in the actual volumes delivered, a 60-mL compliance syringe filled with 30 mL of medium was attached to the system. Fresh medium used for perfusion was stored outside the incubator in an insulated container on ice. Before manual "infusion" of large amounts of fresh medium, the medium was placed on the bench and allowed to equilibrate to room temperature. Additions of small amounts of fresh medium were directly taken from the cooled container. The waste container was placed on the bench outside the incubator at all times without any temperature control.

## Reference Analysis

Glucose and lactate concentrations in samples drawn from the cultures were measured with an analyzer (Model 2700, YSI, Yellow Springs, OH) as detailed by Rhiel et al. (2002a). Glutamine was analyzed using a high-performance liquid chromatography (HPLC) system by a method adapted from Jones and Gilligan (1983), as described by Rhiel et al. (2002a). Ammonia was analyzed with a solid-state diffuse reflectance based fiber-optic sensor as described by Spear et al. (1998) and Rhiel et al. (2002a).

## Spectrometer

Single-beam spectra were collected with a Nicolet Magna 550 FTIR spectrometer (Nicolet, Madison, WI) equipped with a 50-W tungsten-halogen source CaF<sub>2</sub> beamsplitter, liquid-nitrogen-cooled InSb detector, and a multilayer optical interference filter (Barr Associates, Westford, MA) to isolate the range 5000 to 4000 cm<sup>-1</sup>. Spectra were collected through a thermostated transmission cell (Wilmad, Buena, NJ) adjusted to a 1.5-mm pathlength. On-line monitoring was accomplished by directing the spent medium from the pRWV through the transmission cell and back to the suction side of the recirculation pump (Fig. 1). The line carrying the spent medium to the spectrometer was size 14 silicone tubing (Cole Palmer, Vernon Hills, IL) (nominal

inner diameter [i.d.] = 1.6 mm), approximately 140 cm in length. The spectrometer was located next to the 37°C incubator at room temperature. To minimize heat loss during transport of the spent medium to the spectrometer, the 95-cm portions of lines running outside the incubator were insulated with 25/50 3/8 in. i.d. × 3/8 in. nominal wall NP77 tubing.

Spectra collection was automated by placing the initiation of the appropriate spectrometer acquisition software commands of OMNIC v3.1a (Nicolet, Madison, WI) under the control of a VISUALBASIC v4.0 (Microsoft, Seattle, WA) program using Nicolet's MACRO/PRO package. Generally, every 2 h three spectra were collected at 4-cm<sup>-1</sup> resolution and 256 coadded scans, which required 2 min of collection time per spectra. Initial analysis of the spectra and calibration model development have been detailed elsewhere (Rhiel et al., 2002a). Fourier filtering of spectra was adapted from Hazen et al. (1994). In brief, single-beam spectra were transformed into the digital frequency domain. Then a Gaussian-shaped curve was selected based on digital mean and digital standard deviation and used to multiply the spectra in the digital frequency domain. The position of the filter in terms of mean and standard deviation dictated the transmitted information. Spectral noise corresponds to high frequencies and baseline drifts were represented as low frequencies. Proper selection of the filter minimized the magnitude of both high- and low-frequency variations while transmitting analyte-specific information.

The parameters may vary for each analyte of interest and with spectral range used for analysis. In this study, the Fourier-filter parameters were optimized with a subset of the spiked calibration sample spectra for each PLS factor and for each analyte. The previously optimized analyte-specific spectral range was kept constant for the respective analyte. The filter parameters found to be optimum for each number of PLS factors were subsequently used in building a PLS calibration model with all spiked samples and applied to the tissue culture samples validation set. Thus, this set served as a monitoring set in the Fourier-filter optimization. The optimum number of factors was chosen when the standard error of monitoring (SEM) was at a minimum. The set of optimum Fourier-filter parameters, optimum number of PLS factors, and optimum spectral range were then used as input parameters for the spiked samples calibration set and applied to the on-line-collected spectra.

## RESULTS AND DISCUSSION

### Batch Operation of the pRWV

As previously described, the culture medium in the pRWV was recirculated through the oxygenator and spectrometer flowcell at 16 mL/min (Fig. 1). This occurred in a closed-loop as long as no fresh medium was added (infused) and spent (waste) medium withdrawn. Thus, the closed-loop

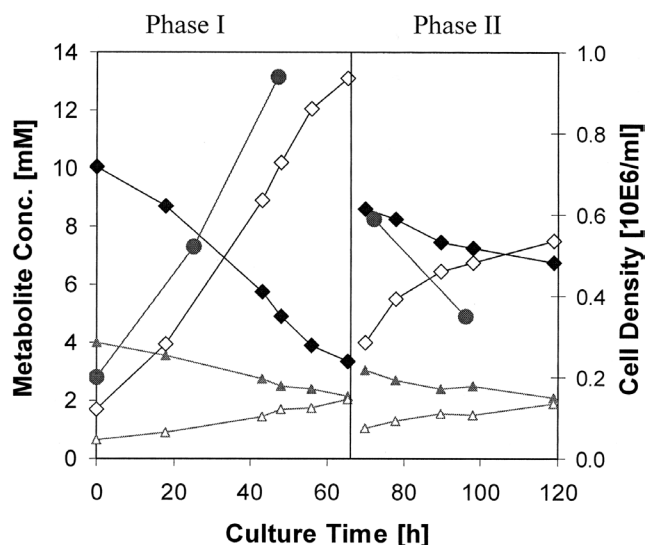


**Figure 2.** Viable cell density (●) and metabolite profiles of glucose (◆), lactate (◇), glutamine (▲), and ammonia (△) during cultivation of PC-3 human prostate cancer cells in an RWV operated in a batch mode after inoculation (phase I) and after partial medium exchange via infusion (phase II). (The metabolite values were measured off-line with the reference methods indicated in the Materials and Methods section).

operation of the pRWV can be considered a “batch” operation. The pRWV was set up from the manufacturer for manual “infusion” of fresh medium. This was accomplished by opening the valves of the manifold to allow “infusion” of fresh medium and at the same time directing spent medium to an outside waste container (dashed lines in Fig. 1). Once the desired amount of fresh medium was added, the valves were closed to continue operation in the closed loop (i.e., batch mode). Operations involving segregated “infusions” of fresh medium may also be considered as “intermittent fed-batch” operation.

Figure 2 shows cell growth and the metabolite profile of PC-3 cells cultivated in a pRWV with one “infusion” of 320 mL of fresh medium over 20 min at the 68-h culture time. Before and after the “infusion,” the pRWV was operated in “batch” mode, resulting in two batch phases (Fig. 2). In the first “batch” phase, PC-3 human prostate cancer cells were inoculated at a viable density of  $0.2 \times 10^6$  cells/mL (Fig. 2). From the concentration profile obtained after sample withdrawal and off-line analysis by the reference analysis approaches described in the Materials and Methods section, the kinetic rates of growth, nutrient consumption, and waste product accumulation could be estimated. As the cells grew at a rate of  $0.033 \text{ h}^{-1}$ , or 21.0-h population doubling time (Table I), glucose and glutamine were consumed as nutrients at  $6.8$  and  $1.8 \times 10^{-17} \text{ mol/cell-s}$ , respectively (Table I). Lactate and ammonia accumulated as waste products of the cellular metabolism at  $11.9$  and  $1.3 \times 10^{-17} \text{ mol/cell-s}$ , respectively (Table I). As lactate results from the glucose metabolism and ammonia from the glutamine metabolism, it was also possible to estimate the metabolic ratio (yields) of these metabolites by plotting the measured lactate concentrations versus the measured

**Table I.** Estimated metabolic rates of PC-3 human prostate cancer cells cultivated in an RWV during batch-phase operation.

Parameter	Unit	Rate
Cell growth	$\text{h}^{-1}$	0.033
Population doubling	h	21.0
Specific glucose uptake	$10^{-17} \text{ mol/cell-s}$	-6.8
Specific lactate production	$10^{-17} \text{ mol/cell-s}$	11.9
Specific glutamine uptake	$10^{-17} \text{ mol/cell-s}$	-1.8
Specific ammonia uptake	$10^{-17} \text{ mol/cell-s}$	1.3

glucose concentrations (Fig. 3a) and ammonia versus glutamine concentrations (Fig. 3b). Clearly, these analytes were correlated, with yields of 1.7 and 0.7 mol/mol for lactate/glucose and ammonia/glutamine, respectively (Table II). These values are comparable to those obtained when PC-3 cells were cultivated in T-150 tissue culture flasks (Fig. 3 and Table II), which suggests that the metabolism was similar in both culture systems.

At the 68-h culture time, fresh medium was “infused” at 16 mL/min for 20 min and the spent medium was directed to the waste container. Two hours after “infusion,” the metabolites were measured with the reference methods to be 8.61, 3.04, 3.98, and 1.03 mM for glucose, glutamine,

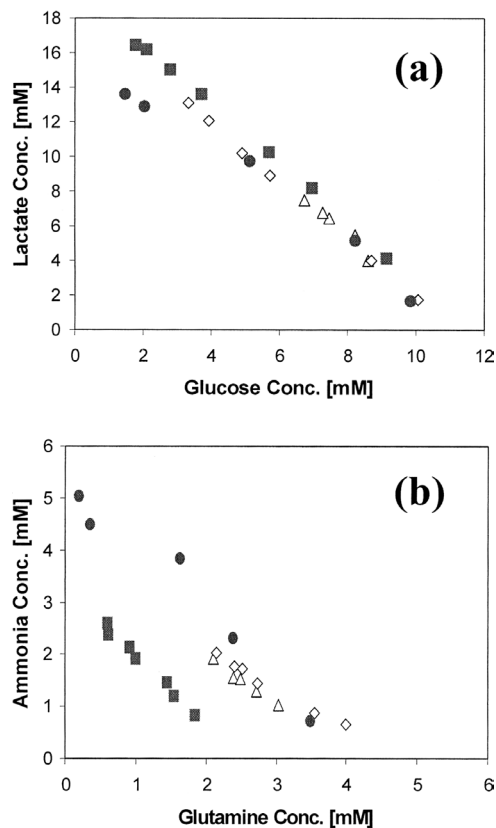


**Figure 3.** Ratios (yields) of lactate produced to glucose consumed (a) and ammonia produced to glutamine consumed (b) during batch phases of the following cultivations: RWV batch run phase 1 (◇); RWV batch run phase 2 (△); RWV perfusion run (■), and cultivation in a T-150 tissue culture flask (●).

**Table II.** Metabolic ratios (yields) during batch cultivation of PC-3 human prostate cancer cells in different cultivation systems and at different phases of the cultivation process.

Culture system and phase	Lactate/glucose yield (mol/mol)	Ammonia/glutamine yield (mol/mol)
T-150 <sup>a</sup> , complete batch	1.7	1.2
RWV, batch run, phase I <sup>a</sup>	1.7	0.7
RWV, batch run, phase II <sup>b</sup>	1.8	0.9
RWV, perfusion run, batch phase <sup>c</sup>	1.7	1.3

<sup>a</sup>T-150: tissue culture flask with a surface of 150 cm<sup>2</sup> (Rhiel et al., 2002a).

<sup>b</sup>See Figure 2.

<sup>c</sup>See Figure 5.

lactate, and ammonia, respectively (Fig. 2). Thus, the starting concentrations at phase II were similar to the

starting concentrations at phase I (Fig. 2). After “infusion” it was expected that the cells continue to grow. However, the cell count at 71.5 h of  $0.59 \times 10^6$  cells/mL was less than the viable density of  $0.94 \times 10^6$  cells/mL at the 47-h culture time (Fig. 2). In fact, the viability dropped and viable cell density continued to decrease further (Fig. 2). As a result, the metabolite changes were smaller (Fig. 2). Nevertheless, the metabolic ratios (yields) remained similar (Fig. 3 and Table II), suggesting that the cellular activity of the remaining cells stayed the same. A possible reason for the decrease in viable cell density could be a washout of free suspended cells during the “infusion” of fresh medium and corresponding withdrawal of spent medium. As the inner cylinder of the pRWV was covered with a 100- $\mu$ m mesh size polypropylene filter to retain cells attached to microcarriers, free suspended cells were not retained, as the mean population diameter of

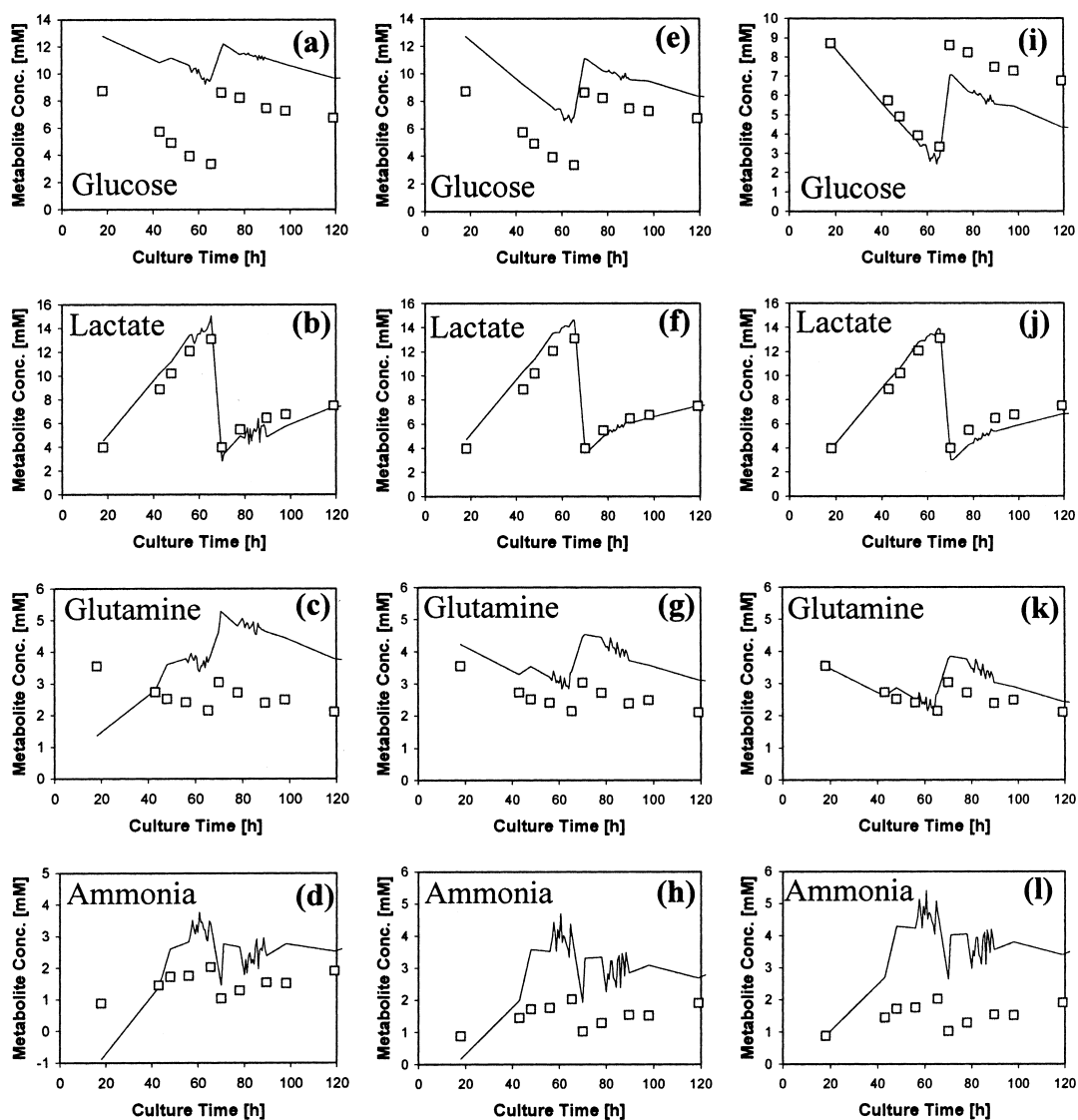


**Figure 4.** Application of various NIR calibration models to on-line monitoring of a RWV batch run. All spectra for calibration model development were collected from tissue culture flask samples (Rhiel et al., 2002a). Application for these off-line-established calibration models to the present RWV batch run were as follows: unfiltered calibration model (a-d), Fourier filtered calibration model (e-h), and Fourier filtered and off-set adjusted calibration model (i-l). Open symbols represent values obtained by off-line reference analysis and solid lines are values obtained by on-line NIR monitoring.

PC-3 cells was approximately 16  $\mu\text{m}$  (determined with a Coulter counter channelyzer). Thus, free suspended cells could easily pass through the filter and may have been washed out. This hypothesis was supported by measuring  $8 \times 10^4$  cells/mL in the waste container after termination of the experiment. The exact washout cell number may have been higher than  $8 \times 10^4$  cells/mL, because some cells probably disintegrated during the time in the waste container, which was at room temperature.

### Calibration Adjustments for On-Line Monitoring

Calibration models for glucose, lactate, glutamine, and ammonia analysis from NIR spectra had been established prior to on-line monitoring and were discussed by Rhiel et al. (2002a). In brief, the calibration models were established using randomly spiked off-line tissue culture samples. This adaptive calibration approach has been shown to yield more robust calibration models (Rhiel et al., 2002c). Figure 4a–d shows the direct application of the NIR calibration models developed by Rhiel et al. (2002a) for glucose, lactate, glutamine, and ammonia on-line monitoring of the aforementioned pRWV culture. It can be seen that the lactate model applied to the on-line-collected spectra resulted in a good estimate of the concentrations (Fig. 4b), resulting in a standard error of prediction (SEP) of 1.03 mM (Table III). Direct application of the glucose model resulted in on-line prediction of concentration values higher than the actual concentrations (Fig. 4a), resulting in an SEP of 4.52 mM (Table III). However, the trend of the glucose profile was accurately predicted; that is, glucose started out at a higher concentration and concentrations decreased during the time course of the batch phase (Fig. 4a). Direct application of the glutamine and ammonia models resulted in inaccurate on-line predictions with SEPs of 1.75 and 1.09 mM for glutamine and ammonia, respectively (Table III).

On-line spectra were usually collected while the medium was recirculating through the system. It was observed by Hazen et al. (1994) that the single-beam spectra of aqueous solutions collected in the 5000- to 4000- $\text{cm}^{-1}$  spectral range do shift to higher frequencies with increasing temperature. Such temperature variations may be present for the on-line-collected spectra as compared with the off-line-collected spectra used to establish the calibration model (Rhiel et al.,

**Table IV.** Summary of PLS calibration model statistics after Fourier filtering of the off-line-collected tissue culture flask samples (Rhiel et al., 2002a) from cultures of PC-3 cells.

Analyte	Spectral range [ $\text{cm}^{-1}$ ]	Fourier filtered mean	Fourier filtered SD	Number of PLS factors	SEC <sup>a</sup> (mM)
Glucose	4450–4300	0.0425	0.0100	4	0.65
Glutamine	4590–4550	0.0300	0.0055	1	0.67
Lactate	4350–4320	0.0500	0.0120	1	0.75
Ammonia	4720–4530	0.0415	0.0100	4	0.65

<sup>a</sup>Standard error of calibration (SEC).

2002a). Digital Fourier filtering of spectra prior to PLS regression analysis has been shown to permit removal of baseline shifts caused by differences in solution temperature (Hazen et al., 1994). In fact, a temperature-insensitive measurement could be performed. To test the potential benefit of Fourier filtering, a similar methodology for optimizing the Fourier-filter parameters was used in this study, as described by Hazen et al. (1994) (see Materials and Methods). Results are summarized in Table IV.

Optimizing the filter parameters maximizes the transmission of analyte-specific information. It can be seen in Table IV that the mean position as well as the standard deviations of the filters are different. For all analytes the number of factors could be reduced. Glutamine and lactate models required only one PLS factor. Fourier filtering did not significantly improve the SEC values or the SEP values of the tissue culture sample validation set.

Application of the calibration models from the Fourier-filtered tissue culture spectra to the previously discussed pRWV culture resulted in further improvement of the on-line lactate predictions (Fig. 4f, Table III), the on-line glucose predictions (Fig. 4e, Table III), and the on-line glutamine predictions (Fig. 4g, Table III). In fact, the on-line glutamine predictions showed a profile trend similar to the actual concentration profile (Fig. 4g). Nevertheless, biases in the absolute concentration values were still present for glucose (Fig. 4e) and glutamine (Fig. 4g). Ammonia predictions, on the other hand, did not improve for on-line monitoring (Table III). This could be due to the fact that the ammonia absorbance feature, which is just one broad peak (Rhiel et al., 2002a), is not as distinct as the absorbance features of the other analytes, which

**Table III.** Summary of on-line standard prediction errors (SEPs) when a priori and off-line-established PLS calibration models were applied to the corresponding referenced on-line-collected spectra during cultivation of PC-3 cell cultures in an RWV.<sup>a</sup>

Analyte	SEP when the unfiltered calibration model is applied to RWV batch run (mM)	SEP when the Fourier filtered calibration model is applied to RWV batch run (mM)	SEP when the Fourier filtered and off-set adjusted calibration model is applied to RWV batch run (mM)	SEP when the Fourier filtered and off-set adjusted calibration model is applied to RWV perfusion run (mM)
Glucose	4.52	2.83	1.62 (4.00)	0.95 (1.50)
Glutamine	1.75	1.19	0.53 (0.68)	0.39 (1.86)
Lactate	1.03	0.90	0.83 (0.72)	0.74 (–0.10)
Ammonia	1.09	1.54	2.13 (–0.71)	1.32 (0.32)

<sup>a</sup>Basic calibration model and subsequent adjustments are detailed in text (corrected initial off-set is indicated in parentheses for the corresponding cultures).

have multiple peaks and narrower absorbance bands (Rhiel et al., 2002a).

When calibration models from off-line-collected spectra are established at some time prior to the application of these models to on-line-collected spectra, instrumental variations may have occurred. In the case discussed by Rhiel et al. (2002b), off-sets could be attributed to differences in instrument alignment. The observed off-sets, however, were constant throughout each complete culture. Rhiel et al. (2002b) showed that subtraction of the initial on-line prediction off-set resulted in accurate concentration predictions throughout the culture progression. The present situation is similar in that calibration models were established a priori with off-line-collected spectra. For collection of off-line spectra, the flow-through cell was removed out of the flow path for each sample exchange. Collection of the spectra occurred after equilibration of the sample in the flow-through cell. For the purpose of collecting off-line spectra, the flow-through cell was charged with just the sample solution (approximately 2 mL). For the purpose of collecting on-line spectra, the complete recycle stream of the pRWV was passed through the flow-through cell, as discussed in Materials and Methods and illustrated in Figure 1. The physical difference between the two collection methods could result in slight alignment shifts.

The on-line predictive ability of the calibration models based on Fourier-filtered spectra (Fig. 4l–k) was greatly improved by adopting the methodology of initial off-set correction from Rhiel et al. (2002b). The initial off-sets observed and the SEP values resulting after adjustment are summarized in Table III. No improvement was achieved for the on-line prediction of ammonia values (Fig. 4l, Table III) as the inaccuracies from model predictions were not due to a constant bias (Fig. 4h). Because all the other results were improved, it was decided to monitor subsequent pRWV cultures on-line with the combination of Fourier-filtered spectra and initial off-set correction.

### Perfusion Operation of the pRWV

The pRWV was extended to continuous perfusion by connecting a low-flowrate pump (Fig. 1). Different perfusion rates and operation modes were investigated subsequently, resulting in four distinct phases (Fig. 5). Phase I took place during the 0- to 50-h culture time when the pRWV was perfused at 0.09 mL/min, corresponding to approximately one reactor volume per day (Fig. 5a). After having turned off the perfusion from 50 to 73 h of culture time (phase II, Fig. 5), perfusion was resumed at 0.17 mL/min (2 reactor volumes per day) from 73 to 149 h (phase III, Fig. 5). Thereafter, the pRWV was operated in batch mode until termination at 266 h of culture time (phase IV, Fig. 5), with a partial medium exchange (100 mL) at 174 h of culture time (Fig. 5).

On-line monitoring of this culture was performed with the calibration model built from Fourier-filtered spectra of off-line samples that were modified using an initial off-set

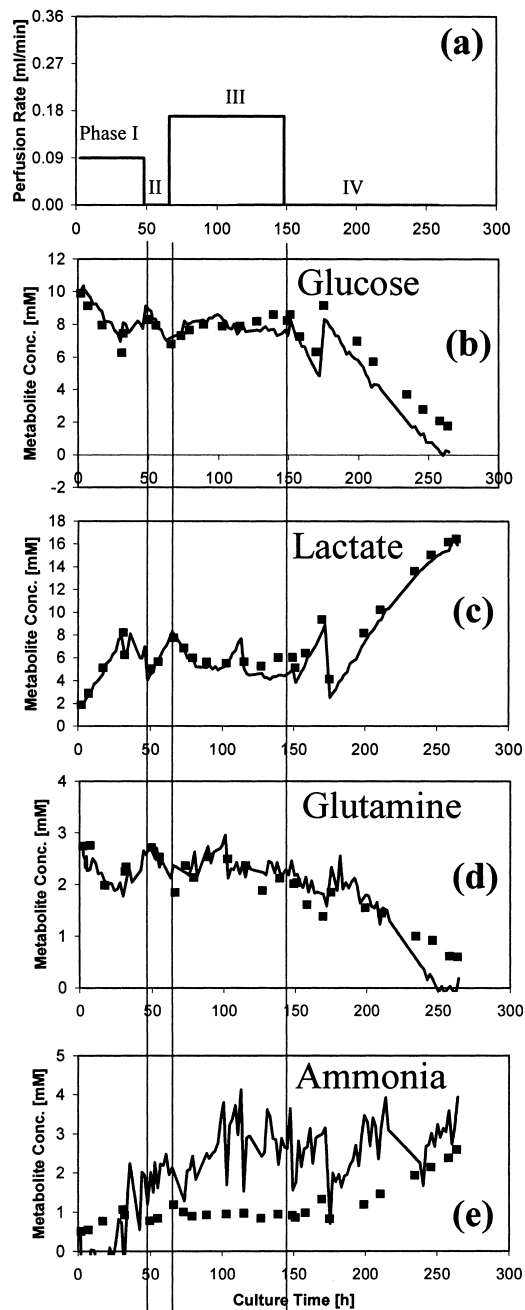


**Figure 5.** Metabolite and perfusion profile of PC-3 human prostate cancer cells cultivated in an RWV as determined using off-line-analyzed reference samples and on-line-obtained concentration values from NIR spectroscopic monitoring using initial offset correction of Fourier-filtered spectra.

adjustment. Using this strategy, glucose, lactate, and glutamine could be monitored with SEPs of 0.95, 0.74, and 0.39 mM, respectively (Table III). Thus, monitoring performance for these analytes during the 266-h continuous perfusion run was similar to the previously discussed 120-h repeated batch run (Table III). As before, it was not possible to monitor ammonia, which could be attributed to the low concentration values and the broad, nondistinct spectral ammonia feature (Rhiel et al., 2002a).

Closer examination of the on-line-monitored metabolite profile for the discussed pRWV run reveals that the monitoring accuracy was highest for lactate throughout the complete run (Fig. 5c). Monitoring accuracy for glucose (Fig. 5b) and glutamine (Fig. 5d) was good throughout phases I, II, and III. During phase IV, however, an increasing bias for both glucose (Fig. 5b) and glutamine (Fig. 5d) appeared. The cause of this bias could not be specified. Its occurrence was similar to the bias observed in the repeated batch runs (Fig. 4i,k) after medium exchange. Its identification requires further experimentation.

From a cell physiology standpoint, perfusion operation with the standard medium at approximately one reactor volume per day was not adequate to supply sufficient medium for keeping the concentrations constant (phase I, Fig. 5). The glucose concentration decreased and the lactate concentration increased (phase I, Fig. 5). After increasing the perfusion rate to two reactor volumes per day at 73 h, a steady state could be achieved (phase III, Fig. 5). Upon resuming batch operation at 149-h culture time, glucose concentrations decreased (Fig. 5b) and lactate concentrations increased (Fig. 5c). In fact, the metabolic yield during this batch phase (phase IV, Fig. 5) was similar to the metabolic yields of the previous batch cultures (Fig. 3a), suggesting that the metabolism remained similar.

Further study of the PC-3 cell metabolism under long-term perfusion operation is needed. The experimental set-up used here would aid in this regard as the key metabolites could be monitored satisfactorily. In fact, timely separation of calibration model establishment with off-line-collected spectra and later application to maintenance-free on-line monitoring would allow calibration on earth and later convenient monitoring during spaceflights. However, further study of bias prevention is needed. Nevertheless, the results presented herein are an important step toward better in vitro models of in vivo behavior.

## CONCLUSIONS

Glucose, lactate, and glutamine concentrations could be predicted from on-line NIR spectra of PC-3 human prostate cancer cell cultures using PLS regression analysis with calibrations performed on a spiked tissue culture sample set. The ammonia concentration could not be measured accurately from the same spectra. Metabolite uptake and production rates were determined for PC-3 prostate cancer cells during exponential growth in batch-mode cultivations. NIR spectroscopy may become a primary sensor mechanism for monitoring the key nutrients, glucose and glutamine, and the cellular waste product, lactate, during continuous perfusion operations of the RWV. This technology is particularly useful for spaceflights as the calibration could be performed on earth and applied in a reagentless, low-maintenance, user-friendly way during such spaceflights. In fact, Rhiel et al. (2002b) showed that calibration models similar to those discussed in this work were still accurate after a 2.3-year period. The only maintenance required

during this period was refilling the detector with liquid nitrogen for cooling. Incorporation of the concentration information into closed-loop control schemes (as reported by Valentinotti et al., 2003) may result in maintaining the constant metabolite concentrations required to better simulate in vivo conditions in vitro.

## References

- Baker TL, Goodwin TJ. 1997. Three-dimensional culture of bovine chondrocytes in rotating-wall vessels. *In Vitro Cell Dev Biol Anim* 33:358–365.
- Bursac N, Papadaki M, Cohen RJ, Schoen FJ, Eisenberg SR, Carrier R, Vunjak-Novakovic G, Freed LE. 1999. Cardiac muscle tissue engineering: Toward an in vitro model for electrophysiological studies. *Am J Physiol Heart Circ Physiol* 277:H433–H444.
- Cavinato AG, Mayes DM, Ge Z, Callis JB. 1990. Noninvasive method for monitoring ethanol in fermentation processes using fiber-optic near-infrared spectroscopy. *Anal Chem* 62:1977–1982.
- Chung H, Arnold MA, Rhiel M, Murhammer DW. 1996. Simultaneous measurements of glucose, glutamine, ammonia, lactate and glutamate in aqueous solutions by near-infrared spectroscopy. *Appl Spectrosc* 50:270–276.
- Chopra V, Dinh TV, Hannigan EV. 1997. Three-dimensional endothelial–tumor epithelial cell interactions in human cervical cancers. *In Vitro Cell Dev Biol Anim* 33:432–442.
- Clejan S, O'Connor KC, Cowger NL, Cheles MK, Haque S, Primavera AC. 1996. Effects of simulated microgravity on DU 145 human prostate carcinoma cells. *Biotechnol Bioeng* 50:587–597.
- Clejan S, O'Connor K, Rosenweig N. 2001. Tri-dimensional prostate cell cultures in simulated microgravity and induced changes in lipid second messengers and signal transduction. *J Cell Mol Med* 5:60–73.
- Colvin GA, Lambert JF, Carlson JE, McAuliffe CI, Abedi M, Quesenberry PJ. 2002. Rhythmicity of engraftment and altered cell cycle kinetics of cytokine-cultured murine marrow in simulated microgravity compared with static cultures. *In Vitro Cell Dev Biol Anim* 38:343–351.
- Cooper D, Pellis NR. 1998. Suppressed PHA activation of T lymphocytes in simulated microgravity is restored by direct activation of protein kinase C. *J Leuk Biol* 63:550–562.
- Cooper D, Pride MW, Brown EL, Risin D, Pellis NR. 2001. Suppression of antigen-specific lymphocyte activation in modeled microgravity. *In Vitro Cell Dev Biol Anim* 37:63–65.
- Duke PJ, Daane EL, Montufar-Solis D. 1993. Studies of chondrogenesis in rotating systems. *J Cell Biochem* 51:274–282.
- Duke J, Daane E, Arizpe J, Montufar-Solis D. 1996. Chondrogenesis in aggregates of embryonic limb cells grown in a rotating wall vessel. *Adv Space Res* 17:289–293.
- Fang A, Pierson DL, Koenig DW, Mishra SK, Demain AL. 1997a. Effect of simulated microgravity and shear stress on microcin B17 production by *Escherichia coli* and on its excretion into the medium. *Appl Environ Microbiol* 63:4090–4092.
- Fang A, Pierson DL, Mishra SK, Koenig DW, Demain AL. 1997b. Secondary metabolism in simulated microgravity: Beta-lactam production by *Streptomyces clavuligerus*. *J Indust Microbiol Biotechnol* 18:22–25.
- Fang A, Pierson DL, Mishra SK, Demain AL. 2000. Relief from glucose interference in Microcin B17 biosynthesis by growth in a rotating-wall bioreactor. *Lett Appl Microbiol* 31:39–41.
- Francis KM, O'Connor KC, Spaulding GF. 1997. Cultivation of fall armyworm ovary cells in simulated microgravity. *In Vitro Cell Dev Biol Anim* 33:332–336.
- Ge Z, Cavinato AG, Callis JB. 1994. Noninvasive spectroscopy for monitoring cell density in a fermentation process. *Anal Chem* 66:1354–1362.
- Glacken MW, Fleischaker RJ, Sinskey AJ. 1986. Reduction of waste product excretion via nutrient control: Possible strategies for maximizing

- product and cell yields on serum in cultures and mammalian cells. *Biotechnol Bioeng* 28:1376–1389.
- Goodwin TJ, Jessup JM, Wolf DA. 1992. Morphologic differentiation of colon carcinoma cell lines HT-29 and HT-29KM in rotating-wall vessels. *In Vitro Cell Dev Biol* 28A:47–60.
- Goodwin TJ, Prewett TL, Spaulding GF, Becker JL. 1997. Three-dimensional culture of a mixed müllerian tumor of the ovary: Expression of in vivo characteristics. *In Vitro Cell Dev Biol Anim* 33:366–374.
- Granet C, Laroche N, Vico L, Alexandre C, Lafage-Proust MH. 1998. Rotating-wall vessels, promising bioreactors for osteoblastic cell culture: Comparison with other 3D conditions. *Med Biol Eng Comput* 36:513–519.
- Hall JW, McNeil B, Rollins MJ, Draper I, Thompson BG, Macaloney G. 1996. Near-infrared spectroscopic determination of acetate, ammonium, biomass, and glycerol in an industrial *Escherichia coli* fermentation. *Appl Spectrosc* 50:102–108.
- Hazen KH, Arnold MA, Small GW. 1994. Temperature-insensitive near-infrared spectroscopic measurement of glucose in aqueous solutions. *Appl Spectrosc* 48:477–483.
- Ingram M, Tegy GB, Saroufeem R, Yazan O, Narayan KS, Goodwin TJ, Spaulding GF. 1997. Three-dimensional growth patterns of various human tumor cell lines in simulated microgravity of a NASA bioreactor. *In Vitro Cell Dev Biol Anim* 33:459–466.
- Jeevarajan AS, Vani S, Taylor TD, Anderson MM. 2002. Continuous pH monitoring in a perfused bioreactor system using an optical pH sensor. *Biotechnol Bioeng* 78:467–472.
- Jessup JM, Brown K, Ishii S, Ford R, Goodwin TJ, Spaulding G. 1994. Simulated microgravity does not alter epithelial cell adhesion to matrix and other molecules. *Adv Space Res* 14:71–76.
- Jones BN, Gilligan JP. 1983. *O*-phthalaldehyde precolumn derivatization and reversed-phase high-performance liquid chromatography of polypeptide hydrolysates and physiological fluids. *J Chromatogr* 266:471–482.
- Klement BJ, Spooner BS. 1993. Utilization of microgravity bioreactors for differentiation of mammalian skeletal tissue. *J Cell Biochem* 51:252–256.
- Lelkes PI, Galvan DL, Hayman GT, Goodwin TJ, Chatman DY, Cherian S, Garcia RM, Unsworth BR. 1998. Simulated microgravity conditions enhance differentiation of cultured PC12 cells towards the neuroendocrine phenotype. *In Vitro Cell Dev Biol Anim* 34:316–325.
- Lewis CB, McNichols RJ, Gowda A, Coté GL. 2000. Investigation of near-infrared spectroscopy for periodic determination of glucose in cell culture media in situ. *Appl Spectrosc* 54:1453–1457.
- Licato LL, Grimm EA. 1999. Multiple interleukin-2 signaling pathways differentially regulated by microgravity. *Immunopharmacology* 44:273–279.
- Long JP, Hughes JH. 2001. Epstein–Barr virus latently infected cells are selectively deleted in simulated-microgravity cultures. *In Vitro Cell Dev Biol Anim* 37:223–230.
- Long JP, Pierson S, Hughes JH. 1998. Rhinovirus replication in HeLa cells cultured under conditions of simulated microgravity. *Aviat Space Environ Med* 69:851–856.
- Margolis L, Hatfill S, Chuaqui R, Vocke C, Emmert-Buck M, Linehan WM, Duray PH. 1999. Long term organ culture of human prostate tissue in a NASA-designed rotating wall bioreactor. *J Urol* 161:290–297.
- Margolis LB, Fitzgerald W, Glushakova S, Hatfill S, Amichay N, Baibakov B, Zimmerberg J. 1997. Lymphocyte trafficking and HIV infection of human lymphoid tissue in a rotating wall vessel bioreactor. *AIDS Res Hum Retrovir* 13:1411–1420.
- McShane MJ, Coté GL. 1998. Near-infrared spectroscopy for determination of glucose, lactate, and ammonia in cell culture media. *Appl Spectrosc* 52:1073–1078.
- Molnar G, Schroedl NA, Gonda SR, Hartzell CR. 1997. Skeletal muscle satellite cells cultured in simulated microgravity. *In Vitro Cell Dev Biol Anim* 33:386–391.
- O'Connor KC, Enmon RM, Dotson RS, Primavera AC, Clejan S. 1997. Characterization of autocrine growth factors, their receptors and extracellular matrix present in three-dimensional cultures of DU 145 prostate carcinoma cells grown in simulated microgravity. *Tissue Eng* 3:161–171.
- Ontiveros C, McCabe LR. 2003. Simulated microgravity suppresses osteoblast phenotype, Runx2 levels and AP-1 transactivation. *J Cell Biochem* 88:427–437.
- Qiu QQ, Ducheyne P, Ayyaswamy PS. 1999. Fabrication, characterization and evaluation of bioceramic hollow microspheres used as microcarriers for 3-D bone tissue formation in rotating bioreactors. *Biomaterials* 20:989–1001.
- Qiu QQ, Ducheyne P, Ayyaswamy PS. 2001. 3D bone tissue engineered with bioactive microspheres in simulated microgravity. *In Vitro Cell Dev Biol Anim* 37:157–165.
- Radin S, Ducheyne P, Ayyaswamy PS, Gao H. 2001. Surface transformation of bioactive glass in bioreactors simulating microgravity conditions. Part I: Experimental study. *Biotechnol Bioeng* 75:369–378.
- Rhiel M, Cohen MB, Murhammer DW, Arnold MA. 2002a. Non-destructive near-infrared spectroscopic measurement of multiple analytes in undiluted samples of serum-based cell culture media. *Biotechnol Bioeng* 77:73–82.
- Rhiel M, Ducommun P, Bolzonella I, Marison I, von Stockar U. 2002b. Real-time in-situ monitoring of freely suspended and immobilized cell cultures based on mid-infrared spectroscopic measurements. *Biotechnol Bioeng* 77:174–185.
- Rhiel MH, Amrhein MI, Marison IW, von Stockar U. 2002c. The influence of correlated calibration samples on the prediction performance of multivariate models based on mid-infrared spectra of animal cell cultures. *Anal Chem* 74:5227–5236.
- Riley MR, Arnold MA, Murhammer DW, Walls EL, De la Cruz N. 1998a. Adaptive calibration scheme for quantification of nutrients and byproducts in insect cell bioreactors by near infrared spectroscopy. *Biotechnol Progr* 14:527–533.
- Riley MR, Arnold MA, Murhammer DW. 1998b. Matrix enhanced buffer calibration procedure for multivariate calibration models with near infrared spectra. *Appl Spectrosc* 52:1339–1347.
- Riley MR, Rhiel M, Zhou X, Arnold MA, Murhammer DW. 1997. Simultaneous measurement of glucose and glutamine in insect cell culture media by near infrared spectroscopy. *Biotechnol Bioeng* 55:11–15.
- Rokhlin OW, Cohen MB. 1995. Expression of cellular adhesion molecules on human prostate tumor cell lines. *The Prostate* 26:205–212.
- Rucci N, Migliaccio S, Zani BM, Taranta A, Teti A. 2002. Characterization of the osteoblast-like cell phenotype under microgravity conditions in the NASA-approved rotating wall vessel bioreactor (RWV). *J Cell Biochem* 85:167–179.
- Saarinen MA, Murhammer DW. 2000. Culture in the rotating-wall vessel affects recombinant protein production capabilities of two insect cell lines in different manners. *In Vitro Cell Dev Biol Anim* 36:362–366.
- Sastry KJ, Nehete PN, Savary CA. 2001. Impairment of antigen-specific cellular immune responses under simulated microgravity conditions. *In Vitro Cell Dev Biol Anim* 37:203–208.
- Schwarz RP, Goodwin TJ, Wolf DA. 1992. Cell culture for three-dimensional modeling in rotating-wall vessels: An application of simulated microgravity. *J Tissue Cult Meth* 14:51–57.
- Spear SK, Rhiel M, Murhammer DW, Arnold MA. 1998. Ammonia measurements in mammalian cell culture media with a diffuse reflectance-based fiberoptic ammonia sensor. *Appl Biochem Biotechnol* 75:175–186.
- Sutherland FW, Perry TE, Nasser BA, Wang J, Kaushal S, Guleserian KJ, Martin DP, Vacant JP, Mayer JE Jr. 2002. Advances in the mechanisms of cell delivery to cardiovascular scaffolds: Comparison of two rotating cell culture systems. *ASAIO J* 48:346–349.
- Sytkowski AJ, Davis KL. 2001. Erythroid cell growth and differentiation in vitro in the simulated microgravity environment of the NASA rotating wall vessel bioreactor. *In Vitro Cell Dev Biol Anim* 37:79–83.
- Valentinotti S, Srinivasan B, Holmberg U, Bonvin D, Cannizzaro C, Rhiel M, von Stockar U. 2003. Optimal operation of fed-batch fermentations via adaptive control of overflow metabolite. *Contr Eng Pract* 11:665–674.

- Wang SS, Good TA. 2001. Effect of culture in a rotating wall bioreactor on the physiology of differentiated neuron-like PC12 and SH-SY5Y cells. *J Cell Biochem* 83:574–584.
- Winkenwerder JJ, Murhammer DW, Reece JS, Palechek PL, Saarinen MA, Arnold MA, Cohen MB. 2003. Evaluating prostate cancer cell culturing methods: A comparison of cell morphologies and metabolic activity. *Oncol Rep* 10:783–789.
- Wolf DA, Schwarz RP. 1991. Analysis of gravity-induced particle motion and fluid perfusion flow in the NASA-designed rotating zero-head-space tissue culture vessel. NASA technical paper 3143.
- Wolf DA, Schwarz RP. 1992. Experimental measurement of the orbital paths of particles sedimenting within a rotating viscous fluid as influenced by gravity. NASA technical paper 3200.
- Xu V, Jeevarajan AS, Fay JM, Taylor TD, Anderson MM. 2002. On-line measurement of glucose in a rotating wall perfused vessel bioreactor using an amperometric glucose sensor. *J Electrochemical Soc* 149:H103–H106.
- Yano T, Aimi T, Nakano Y, Tamai M. 1998. Prediction of the concentration of ethanol and acetic acid in the culture broth of a rice vinegar fermentation using near infrared spectroscopy. *J Ferment Bioeng* 85:461–465.
- Zhau HE, Goodwin TJ, Chang SM, Baker TL, Chung LWK. 1997. Establishment of a three-dimensional human prostate organoid coculture under microgravity-simulated conditions: Evaluation of androgen-induced growth and PSA expression. *In Vitro Cell Dev Biol Anim* 33:375–380.
- Zhou X, Chung H, Arnold MA, Rhiel M, Murhammer DW. 1995. Selective measurement of glutamine and asparagine in aqueous media by near-infrared spectroscopy. In: Rogers KR, Mulchandani A, Zhou W, editors. *Biosensor and chemical sensor technology: Process monitoring and control*. ACS symposium series 613. Washington, DC: ACS. p 116–132.
- Zielke HR, Ozand PT, Tildon JT, Sevdalian DA, Cornblath M. 1978. Reciprocal regulation of glucose and glutamine utilization by cultured human diploid fibroblasts. *J Cell Physiol* 95:41–48.